arXiv:astro-ph/0207348v1 16 Jul 2002

Spectroscopic Survey of the Galactic Open Cluster NGC 6871 I. New Emission Line Stars

Zoltan Balog[1] and Scott J. Kenyon

Smithsonian Astrophysical Observatory, 60 Garden Street, Cambridge, MA 02138

zbalog@cfa.harvard.edu and kenyon@cfa.harvard.edu

ABSTRACT

We analyze spectra of 44 emission line stars detected in a low resolution optical spectroscopic survey of the galactic open cluster NGC 6871. The survey of 1217 stars is complete to $V = 14.9$ and includes stars with $V < 16.5$ between the zero age main sequence (ZAMS) and the 10^7 yr pre-main sequence (PMS) isochrone. Of the 44 emission line stars in this survey, 28 show obvious emission in $H\alpha$ and 16 have weak $H\alpha$ absorption (compared to $H\gamma$). We use the reddening to separate foreground and background stars from the cluster members; the position in the HR diagram (HRD) or the presence of forbidden emission lines ([NII], [SII]) then yields the evolutionary status of the emission line stars. A comparison of the $H\alpha$ spectral index distribution in NGC 6871 with the distribution of young stars in the Taurus-Auriga molecular cloud indicates that the late type PMS stars in our sample may be weak line T Tauri stars (wTTs). Many of these stars show [SII] (36%) and [NII] (45%) emission.

Subject headings: clusters: open, stars–spectral types: Be stars

1. Introduction

Establishing mass-and age-dependent color-luminosity relations is important for understanding the physical processes leading from molecular clouds to main sequence stars. As in main sequence and post main sequence stars, observational HR-diagrams for PMS stars allow comparisons between observations and predictions of evolutionary models. Because isochrone fitting allows a more reliable measurement of distances and ages for star clusters than for single stars, the detection of PMS stars as members of star clusters offers an advantage over the observation of individual stars in more extended star forming regions. This advantage leads to accurate colors and luminosities for the possible PMS members of open clusters with well defined constraints on age and mass.

The aim of this paper is to describe 37 new emission line objects along the line of sight to the galactic open cluster NGC 6871. We identify these stars from a program to measure accurate

[1]on leave from Dept. of Optics and Quantum Electronics University of Szeged, Szeged, Hungary

spectral types, to derive the reddening, to separate cluster members from foreground and background stars, and to construct the Hertzsprung-Russell diagram (HRD) for cluster members. We will describe these results in a future paper.

With an age of roughly 10^7 yr, NGC 6871 is at an important stage in the early evolution of an open cluster. Younger clusters with ages of $\sim 10^6$ yr are often embedded in a bright nebulosity or a dark molecular cloud. Most of the young stars in these clusters have circumstellar disks (Haisch et al. 2001). Older star clusters with ages of 10^8 yr have little nebulosity or molecular gas. Few stars in these cluster have disks (Habing et al. 2001; Spangler et al. 2001). In NGC 6871, the lack of significant nebulosity or molecular gas allows optical spectroscopic observations to derive spectral types and luminosities of cluster members, and to measure IR excesses from circumstellar disks. Optical data provide a reliable measurement of the IMF for comparison with other young clusters (e.g., Slesnick et al. 2002). Recent work suggests that circumstellar disks disappear on timescales of 5-10 Myr (Haisch et al. 2001). Observations of IR excess emission in NGC6871 thus yield better constraints on disk timescale.

NGC 6871 has been relatively well studied photometrically. The cluster is part of the Cyg OB3 association (Garmany & Stencel 1992), one of the largest nearby star formation complexes. The most recent UBV CCD photometry published by Massey et al. (1995) has a limiting magnitude $V \simeq 16.5$. Several age estimates exist for the cluster members. From isochrone fitting, Massey et al. (1995) derived ages of 2 - 5 Myr for the stars with $M > 25 M_\odot$ (spectral type B0 and earlier). From uvby photometry for stars with spectral type earlier than B5 ($M > 4 M_\odot$), Reimann (1989) estimated an age of 10 - 20 Myr. The difference between the two ages suggests either a large age spread among the cluster members, contamination from nearby stars in the local spiral arm (Slesnick et al. 2002), or large uncertainties in age estimates derived from optical photometry. The presence of O stars in the cluster sets an upper limit for ages of high mass stars. According to Massey et al. (1995), the highest mass stars in the cluster have $M = 40\ M_\odot$ and main sequence lifetimes of 4-5 Myr (Schaller et al. 1992). However, Massey et al. (1995) note that the cluster contains evolved 15 $M_\odot$ stars with main sequence lifetimes of 11 Myr.

One of the goals of our program is to test the origin of the age difference by deriving accurate spectral types for cluster members. According to the WEBDA catalog of J-C. Mermilliod (Mermilliod 1995), 12 stars in the cluster have reliable spectral types (e.g., Roman 1951; Hiltner 1956; Walborn 1971; Massey et al. 1995). The SIMBAD database lists another 151 stars with spectral classifications in the field of NGC 6871. Only 58 of these stars are included in the photometric database of Massey et al. (1995) from which we selected our spectroscopic candidates. The discrepancy between the numbers of stars with spectral types in different catalogues can be explained by the incompletness of the WEBDA and the uncertain spatial bounderies of the catalogue of Massey et al. (1995). Some stars with spectral type must lie outside the CCD field of Massey et al. (1995). Our sample of 1217 stars will yield a good comparison between ages derived from photometric and spectroscopic techniques. This large sample also provides a good measurement of the frequency of $H\alpha$ and other emission lines as a function of spectral types. Emission lines disappear when disk

accretion ends; our data thus provide an estimate of the time scale for the end of disk accretion for intermediate and low mass stars.

We adopt an automatic approach and measure spectral types from spectral indices derived from digital spectra. This method allows robust measurement of spectral types and can be rapidly applied to large numbers of spectra. The accuracy of the method is comparable to visual estimates. We also use spectral indices to identify emission line objects. We compare the strength of the Hα and Hγ indices and identify an object as emission line star if the Hα absorption is weak relative to Hγ. This method yields an automatic identification of emission line stars in cases where the emission is not obviously detectable by visual examination.

In this first paper of the series we report the discovery of 37 new emission line stars and analyze their spectra. Eight stars with accurate spectral types are known emission line stars (we detect seven of these stars). Here, we extend this sample to 45 stars and begin to separate cluster members from foreground and background stars.

2. Observations

We use the WEBDA for selecting the target stars for our survey and adopt the WEBDA designation for stars throughout this paper. We selected stars from the WEBDA which have reliable UBV CCD photometry. The survey of 1217 stars is complete to $V = 14.9$ and includes stars with $V < 16.5$ between the ZAMS and the 10^7 yr PMS isochrone of Siess et al. (2000).

P. Berlind, M. Calkins, and several other observers acquired low resolution optical spectra of stars on the field of NGC 6871 with FAST, a high throughput, slit spectrograph mounted at the Fred L. Whipple Observatory 1.5-m telescope on Mount Hopkins, Arizona (Fabricant et al. 1998). They used a 300 g mm^{-1} grating blazed at 4750 Å, a 3″ slit, and a thinned Loral 512 × 2688 CCD. These spectra cover 3800–7500 Å at a resolution of $\sim$ 6 Å. We wavelength-calibrate the spectra in NOAO IRAF[2]. After trimming the CCD frames at each end of the slit, we correct for the bias level, flat-field each frame, apply an illumination correction, and derive a full wavelength solution from calibration lamps acquired immediately after each exposure. The wavelength solution for each frame has a probable error of ±0.5–1.0 Å. To construct final 1-D spectra, we extract object and sky spectra using the optimal extraction algorithm within APEXTRACT. Most spectra have moderate signal-to-noise, S/N $\gtrsim$ 30 per pixel.

To measure the spectral types of individual stars, we measure continuum magnitudes and indices using narrow passbands (O'Connell 1973; Worthey et al. 1994). The absorption and emission indices, derived using SBANDS within IRAF, are $I_\lambda = -2.5 \log(F_\lambda/\bar{F})$, where F_λ is the average flux in the passband λ and $\bar{F}$ is the continuum flux interpolated between the fluxes in the neighboring

[2]IRAF is distributed by the National Optical Astronomy Observatory, which is operated by the Association of Universities for Research in Astronomy, Inc. under contract to the National Science Foundation.

blue band centered at λ_b and the red band centered at λ_r. Table 1 lists the indices used in our analysis. We establish relations between indices and spectral type using the standards of Jacoby et al. (1984). We use the sum of the He indices ($I_{He} = I_{He\lambda4144} + I_{He\lambda4387} + I_{He\lambda4471} + I_{He\lambda4922}$) for stars earlier than B2, and two different sums of the H indices ($I_{H1} = I_{H\alpha} + I_{H\beta} + IH\gamma + I_{H\delta} + I_{H\lambda3889} + I_{H\lambda3835}$, $I_{H2} = I_{H\alpha} + I_{H\beta} + I_{H\gamma} + I_{H\delta} + I_{H\lambda3889}$) for stars later than B0. We define two H indices because $H\lambda3835$ is unreliable for stars with spectral type of A2 or later. We use the sum of TiO indices ($I_{TiO} = I_{TiO\lambda5968} + I_{TiO\lambda6182} + I_{TiO\lambda6234} + I_{TiO\lambda7100}$) for stars with detectable TiO bands. We apply three different linear fits to the different parts of the index - ST relation for the hydrogen and the helium indices and a 3rd degree polynomial fit to the TiO index, where ST is the numerical spectral type ($0 = \mathrm{O0}, 10 = \mathrm{B0}, 20 = \mathrm{A0}$ and so on).

To check the reliability of our spectral types, we compare with published types for 58 stars in our sample. We define δST = ST(present paper) - ST(literature), and derive the mean $< \delta\mathrm{ST} > = -0.21 \pm 4.1$. Twelve stars are responsible for most of the dispersion. Checking these types visually, we verify that all of these stars are misclassified. For example, of the three K5 stars in the SIMBAD database, one is an M star with strong TiO bands and two are obvious G-type stars. Removing these misclassifications from the complete sample, we measure $< \delta\mathrm{ST} > = 0.15 \pm 1.7$. An error of 1-2 subclasses is typical of visual classifications (e.g., Cutispoto et al. 1999).

Spectral indices provide an efficient method for deriving spectral types from low resolution digital spectra. As multi-object spectrographs become available on many telescopes, robust digital spectral types are necessary to place cluster HR diagrams on a reliable, repeatable scale. Our technique yields accurate spectral types for stars without emission lines. Because luminosity classification requires higher spectral resolution, this technique does not yield reliable luminosity classes. However, spectral indices are easily generalized to derive luminosity classes on higher resolution spectra. To derive spectral types for emission line stars, we follow Jaschek & Jaschek (1987) and estimate spectral type visually. Based on comparisons with published spectral types, our classification for these stars have an uncertainty of $\pm$ 0.9 subclasses

3. Results

3.1. Selection of emission line stars

We use HI indices to identify emission line stars in our sample. In normal main sequence stars, the HI equivalent widths are a function of spectral type (see e.g., Jaschek & Jaschek 1987). The equivalent widths peak at A2 spectral type, (e.g. $I_{H_\beta} \simeq 0.7$), and decrease towards earlier and later spectral types. All of the HI Balmer lines have roughly equivalent absorption line equivalent widths. In contrast, the equivalent widths of Balmer emission lines depend on the upper level. The relative fluxes for the Hα, Hβ, and Hγ emission lines are roughly 3:1:0.45 (Osterbrock 1989). Thus, HI emission fills in the Hα absorption line before affecting higher members of the Balmer series. We use weak Hα absorption relative to Hβ and Hγ absorption to identify emission line stars with

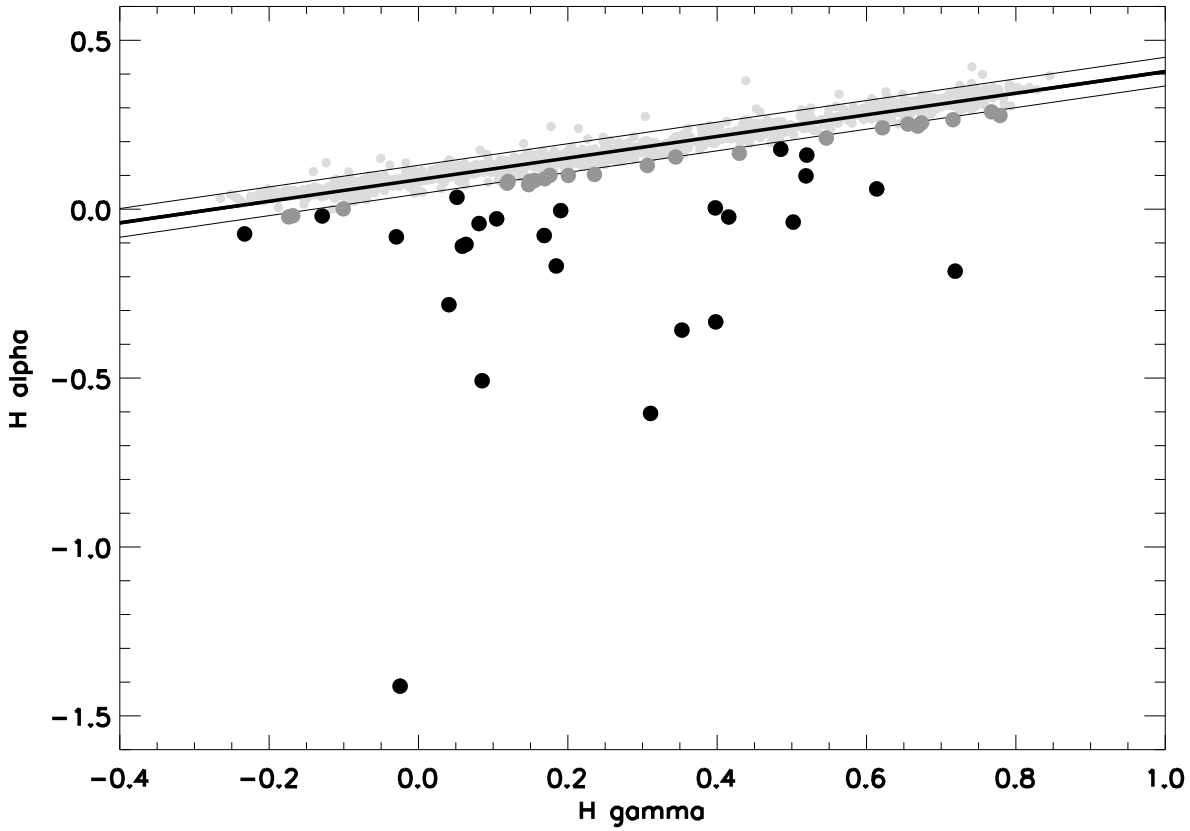

Fig. 1.— $I_{H\alpha}$ vs $I_{H\gamma}$ diagram for stars in the spectroscopic sample. The lines represent the linear relation fitted to the indices (dark line) and the 2σ limits (light lines). Light grey dots denote the normal main sequence stars, grey dots denote the candidate emission line objects, and black dots denote the obvious emission line objects

no obvious $H\alpha$ emission feature (see also Bragg & Kenyon (2002)).

Fig 1. shows the $H\alpha$ index ($I_{H\alpha}$) as a function of the $H\gamma$ index ($I_{H\gamma}$) for our program stars. The majority of the stars follow a straight line with relatively small scatter. These are normal main sequence stars without emission lines. We derive a linear relation between the two indices for these stars with a least squares fit,

$$I_{H\gamma} = 0.32 * I_{H\alpha} + 0.09.$$

The rms of the fit is $\sigma = 0.02$. We make several iterations before accepting the final fit. First we reject the stars with obvious emission lines (negative $H\alpha$ indices). After performing a first fit we eliminate the stars which lie beyond the 2σ limit. This group contains all of the obvious emission line stars and outliers with poor S/N spectra (above the 2σ limit on Fig 1.). Then we perform a final fit and measure the rms of the linear relation for normal stars. We adopt this rms for selecting emission line candidates.

We identify "definite" emission line objects as stars that fall more than 3σ below the straight line fit. Candidate emission line objects fall 2-3σ below the fit. Visual inspection of the spectra confirms that 22/24 of the definite emission line objects and 4/20 of the candidates have obvious $H\alpha$ emission. In the other stars, the $H\alpha$ absorption line is definitely weaker than in normal main sequence stars. Tables 2 and 3 list our sample of 44 emission line stars along with our derived spectral types, reddening, and photometric data from the catalogue of Massey et al. (1995) (MJD95). We also list the designation of the stars from MJD95. Fig. 3 shows the color-magnitude diagram for these stars.

3.2. Analysis of the emission line stars

In this section we derive the reddening $E(B-V)$ of stars in the field of NGC 6871 using their linked photometric and spectroscopic data. Accurate reddening values allow us to filter out foreground and background objects from our sample, and provide a more accurate placement of stars on the HRD.

3.2.1. Reddening and membership

We calculate the $E(B-V)$ for each non-emission line (normal) main sequence star in our sample from the measured spectral type and the color table of Kenyon & Hartmann (1995). Because Kenyon & Hartmann (1995) does not include stars with spectral type earlier than B0, we calculate a lower limit to $E(B-V)$ for these stars and do not include them in the analysis. The left panel of Fig. 2 shows the reddening histogram for normal main sequence stars in the cluster

field. The distribution peaks around $E(B-V) = 0.4$. This value agrees with previous values of $E(B-V) = 0.443$ (WEBDA) and $E(B-V) = 0.46$ (Massey et al. 1995).

We use the reddening calculated by the computer code of Hakkila et al. (1997) to check our results. The Hakkila et al. (1997) program yields visual extinction as a function of Galactic longitude, Galactic latitude, and distance. The code combines the results of published studies (see references in Hakkila et al. (1997)). Three studies (Fitzgerald 1968; Neckel et al. 1980; Arenou et al. 1992) provide information on the reddening for the Galactic coordinates of NGC 6871. Our estimate for $E(B-V)$ agrees only with the results of Neckel et al. (1980). The study of Arenou et al. (1992) overestimates the reddening by a factor of 2; the study of Fitzgerald (1968) underestimates the reddening by a factor of 2. We use the results of Neckel et al. (1980) below.

The right panel of Fig. 2 shows the reddening histogram of emission line stars in the cluster field. The distribution is similar to the histogram for normal stars. However there is an excess of emission line stars with virtually no reddening. These stars may be single young stars in the vicinity of the Sun or part of a nearby young association. Including these zero reddening stars, 22% of the emission line stars seem to belong to the foreground population. The stars with $E(B-V)$ between 0.3 and 0.5 are probably members of the cluster. Roughly 1/3 (38%) of our emission line stars belong to this group. Stars with $E(B-V) > 0.5$ could be background objects. Roughly 40% of the emission line stars has larger reddening than the cluster members. According to the A_v-distance relation of Neckel et al. (1980), these stars have distances larger than 1.9 kpc. The distance can be as large as 6.6 kpc for the highly reddened O star id2905 (HD226868). Such large distances seem improbable, because they imply unreasonably large absolute magnitudes. The calculated z value above the galactic plane ($z > 200$ pc) for id2905 also contrasts with the accepted z values for O - B stars ($50 - 100$ pc), which suggests that this star has extra circumstellar reddening compared to cluster stars. The distances of the other background stars seem reasonable for the position of NGC 6871 but some of these stars might be cluster members with extra reddening due to circumstellar material. We examine this possibility further in the next subsection.

3.2.2. Emission line objects on the cluster Hertzsprung-Russell diagram

Having derived the B-V color excess for the emission line stars, we calculate the A_v and the bolometric correction for each star in our sample and construct the HRD for each subsample specified in the previous section (foreground, cluster, background). Fig 3 shows these diagrams. Fig 3a (top left) shows the HRD for all stars in our sample, Fig 3b (top right) shows the HRD for the cluster; Fig 3c and Fig 3d (bottom left and right) show the HRD of the background and the foreground stars respectively. Small grey dots denote normal main sequence stars; large black dots denote emission line stars. The solid curves show the ZAMS of Siess et al. (2000) shifted with the distance modulus $DM = 11.08$ which corresponds to a distance of 1649 pc (Battinelli & Capuzzo-Dolcetta 1991).

Although the majority of emission line stars in the cluster follow the ZAMS, four emission line stars lie above the main sequence. These objects may be PMS stars (see section 4.). Several other non-emission line objects lie close to these stars in the HRD. The relatively large scatter of these apparent PMS stars in the HRD suggest a large age-spread in the cluster (Massey et al. 1995; Reimann 1989).

The HRD of background objects (Fig 3c) is very similar to the HRD for cluster members. Roughly half of the emission line stars lie on or above the ZAMS, which suggests that they are cluster members with extra reddening due to circumstellar material. Radial velocity measurements would test this possibility.

The stars with lower reddening occupy an area above the main sequence. Most of these stars are foreground objects with different distance moduli. Three of the four zero reddening stars may lie at the same distance: they are on a line nearly parallel to the ZAMS and may be a small group of young stars. The fourth of the unreddened stars may lie within 100 pc but its spectral type is uncertain. Further observations would place better limits on its distance. The other foreground stars lie just above the main sequence. Their position is consistent with the distance calculated from their reddening using the calibration of Neckel et al. (1980) (1.2 kpc). They may be part of another young open cluster along the line of sight to NGC 6871 or a lower density concentration of stars in the local spiral arm.

4. Short description of the spectra of the emission line stars

In this section we give a short description of emission line stars in our sample. We follow the previous section and divide the sample into foreground, background, and cluster stars. In each section, we classify the stars as main sequence or pre-main sequence based on their positions in the HRD, the presence of [NII], [SII] emission lines, and the detection of the Li I λ6708 absorption line. Although Li I λ6708 absorption provides the best age measure for a young star, we detect Li I λ6708 only in a few cases due to the low resolution of our spectra. Even where we detect the Li I λ6708 line, the detection is very uncertain. Higher resolution spectra would provide a better test for the presence of Li I λ6708 in these stars.

With several O-type stars in the cluster, [NII] and [SII] emission lines could result from poor sky/nebula subtraction. To test this possibility, we measure an [SII] index for the complete spectroscopic sample. If fluctuations in nebular emission across the cluster field produce [NII] and [SII] emission, we expect roughly equal numbers of sources with apparent [NII] and [SII] absorption. Our test indicates a small dispersion in $I_{[SII]}$ with $\sigma = 0.01$. We identify a slight trend of increasing [SII] index towards later spectral types. The only exceptions to this trend are [SII] emission line stars. There are no stars with apparent [SII] absorption. Thus, we conclude that nebular contamination is not responsible for the [SII] or [NII] emission line stars.

4.1. Foreground stars

There are 9 stars in our sample with low reddening. Because all are fainter than the Hipparcos limit, we cannot use accurate distances or proper motions to test the evolutionary status of these stars. Most have late spectral types (F - M). One (id2399) has an early spectral type (A2) with very weak emission in the core of the $H\alpha$ line.

There are five F type stars among the foreground objects. Two (id1755, id1552) have visible emission; the other three (id1221, id2545, id1869) show weak $H\alpha$ absorption. These stars have roughly the same distance according to their position on the HRD and the A_v-distance relation of Neckel et al. (1980). This distance coincides with the distance of the majority of the normal foreground stars, suggesting that they may be part of a cluster between the Sun and NGC 6871. Radial velocity measurements would test this idea. Only one of these stars (id1755) is among our PMS candidates.

Two of the remaining three stars (id1647, id1659) might be wTTs with spectral type around K8. All of their Balmer lines are in emission along with the Ca H and K lines. We detect Li I λ6708 line in the spectrum of id1659 even at our low resolution.

There is one M star in our sample (id113) with weak $H\alpha$ and [NII] emission. To examine the possibility that id113 is a dMe star, we estimate the number of nearby dMe stars from the observed stellar density of 0.084 star/pc^{-3} (Henry et al. 2002). Roughly 70% of nearby stars are M dwarfs (Henry et al. 2002). At our completeness limit ($V \simeq 14.9$), we can detect M dwarfs at distances of 100 pc. The number of detectable M dwarfs towards NGC 6871 is two. The number of dMe stars among M dwarfs increases monotonically with spectral type (4% around M0 and 90% M5 and later (Joy & Abt 1974)). The overall ratio of dMe stars among M dwarfs is 17%, which yields a modest probability ($\simeq$ 34%) of detecting one in our spectroscopic sample. Thus, id113 could be a dMe star. High resolution optical spectra of Li I λ6708 would discriminate between a field dMe star and a pre-main sequence star.

4.2. Probable cluster members

There are 15 emission line stars in this group. Their spectral types range from early B to late G. Most are definite emission line objects. More than half of the 15 cluster members (9 altogether) appear to be PMS stars. For 8 stars, we base this identification on their position on the HRD. One star has [NII] and [SII] emission.

There are three B type stars (id8, id186, id38) among the 11 definite emission line stars. They show emission only in $H\alpha$. Two of them (id8 and id38) were previously known (see Grigsby & Morrison 1988; Bernabei & Polcaro 2001). They could be classical Be stars.

There are two A stars (id2139, id1694) in this subgroup. One (id2139) shows signs of [NII]

and [SII] emission. The $H\alpha$ emission of id1694 is very weak, but its position on the HRD indicates that it may be a PMS star.

There are three F type stars with definite emission features among the cluster members. Two (id2646, id2631) are PMS candidates with [NII] and [SII] emission. The third one (id2055) shows emission in $H\alpha$ and lies close to the main sequence.

Three G type members (id2621, id2138, id2675) may be PMS stars. All lie well above the main sequence. The spectrum of id2621 contains [NII] and [SII] emission; we detect Li I λ6708 line in the spectrum of id2138. The third star of this group does not show any particular feature beside the weak emission in the core of the $H\alpha$ line.

4.3. Stars with high reddening

Based on their reddening, we identify 16 emission line stars as possible background objects. The majority are early type objects; only three have spectral type F or later. Roughly half of these stars lie above the ZAMS on the HRD, suggesting that these are probably cluster stars with extra (circumstellar) reddening.

Seven of the stars (id3, id6, id2352, id215, id2209, id1062, id1238) have B spectral types. All have definite emission lines except id3. Two (id1062 and id2209) lie above the main sequence and are included in our PMS candidate sample. In the case of id6 and id1062, the whole Balmer series is in emission; id2352, id215, id2209 and id1238 show detectable emission only in the $H\alpha$ line.

There are six A type stars in this group (id2320, id2492, id1651,id1093, id2637, id2156). Only two (id2320 and id2492) show definite $H\alpha$ emission; four have a weak $H\alpha$ absorption line. We identify four (id2320, id2492, id1651, id2156) as candidate PMS stars according to their position on the HRD. One of these stars (id2320) shows emission in [NII] and [SII]

Because they lie above the main sequence, all of the three late type objects (id1379, id1845, id2245) are among our PMS candidates. Only one (id2245) shows Li I λ6708 absorption line.

5. Comparing PMS candidates with the young stars in the Taurus-Auriga molecular clouds

Walter (1987) and Walter et al. (1988) divide the low mass PMS stars into two groups according to their spectroscopic and photometric properties. Classical T Tauri stars (cTTs) have strong $H\alpha$ emission, with $EW(H\alpha) > 10$Å; wTTs have $EW(H\alpha) < 10$Å. Most cTTs have other strong emission lines from HI, CaII and sometimes HeI. Many have [NII], [SII] and [OI] emission from winds or collimated jets. cTTs also display large infrared excesses from a circumstellar disk. Optical veiling is observable in the spectra of cTTs which indicates the presence of extra emission

from a boundary layer or accretion hot spot (Bertout 1989). wTTs often have CaII and other chromospheric emission lines. They usually have nearly blackbody spectra and rarely display jet or wind emission features (Bertout 1989).

To place our emission line stars in context with other PMS stars, we compare our sample with stars in the well studied Taurus-Auriga cloud (e.g., Kenyon & Hartmann 1995). Fig 4. compares the distribution of the $H\alpha$ indices of T Tauri stars in Taurus-Auriga (Kenyon et al. 1998) with late type PMS stars in the field of NGC 6871. The two histograms peak at the same index value. Compared to Taurus-Auriga, NGC 6871 has few strong emission stars and an overabundance of weak emission line stars.

With age of $\simeq 10^6$ yr, the PMS stars in Taurus-Auriga are much younger than the apparent age ($\simeq 10^7$ yr) of PMS stars in NGC 6871. Observations of other young clusters suggest that the disk accretion which powers cTTs emission declines on timescales of $\simeq 10^7$ yr (Hartmann et al. 1998; Haisch et al. 2001). Our apparent discovery of wTTs in NGC 6871 is consistent with these observations. We plan to return to this issue in future papers where we analyze the non emission line stars in the cluster.

6. Conclusions

We have begun a spectroscopic survey of the galactic open cluster NGC 6871. Our spectra cover $3700 - 7400$Å at $\simeq 6$Å resolution. The survey is complete to $V = 14.9$ and includes stars with $V < 16.5$ between the ZAMS and 10^7 yr PMS isochrone.

Using $H\alpha$ and $H\gamma$ spectral indices, we identify 44 emission line stars. The spectral types of these stars range from O9 - K8; one star may have an M5 spectral type. Eight stars have [NII] emission; six stars have [SII] emission. A few stars may have Li I λ6708 absorption; higher resolution spectra with good signal-to-noise would test these detections.

We use the reddening E_{B-V} to divide the emission line sample into foreground stars, background stars, and cluster members. Nine stars have very low reddening and are probably foreground stars. Eighteen stars are much more highly reddened than the cluster stars. However, most of these lie above the cluster main sequence on the HRD, suggesting that these stars are cluster stars with extra (circumstellar) reddening. We thus conclude that 24 emission line stars are cluster members.

The 9 foreground stars fall into two groups. Four stars have essentially no reddening and are therefore nearby stars with $d \lesssim 300$ pc. These might be part of a nearby association, similar to the TW Hydrae association (de la Reza et al. 1989; Gregorio-Hetem et al. 1992; Zuckerman et al. 2001) or the η Chamaeleontis cluster (Mamajek et al. 1999). The other five stars also appear to lie at the same distance and might form another association or group along the line of sight to NGC 6871.

The emission line stars in the cluster consist of two groups. Stars with spectral type $\lesssim$ A0 lie on the main sequence and have ages of t < 1.4x10^7 yr (Siess et al. 2000). Some of these stars

may be classical Be stars. Near infrared data would allow a test of the evolutionary status of these stars. Lada & Adams (1992) found that PMS Be stars and classical Be stars occupy well-defined, different regions of the J-H, H-K color-color diagram. A few F-type emission line stars may belong to this group. Several stars with spectral types A - G lie above the cluster main sequence and may be PMS stars. The distribution of $H\alpha$ indices for these stars coincides with the peak observed for wTTs in the Taurus-Auriga molecular cloud. If these are PMS stars, they are wTTs not cTTs. Some of these stars show [NII], [SII] emission and may have LiI absorption, which provides some evidence for their PMS status.

The discovery of [SII] and [NII] in apparent wTTs in NGC 6871 is a new and unexpected result of our survey. Previous observations of wTTs in other regions rarely detect [NII] or [SII] emission (Kenyon et al. 1998; Hartigan et al. 1995). We detect [NII] emission in 45% and [SII] emission in 36% of our candidate wTTs; none of these show [OI] emission features in their spectra. In many PMS stars, [OI], [NII], and [SII] emission lines are associated with disk accretion phenomena (e.g. jets and disk-wind interactions; Hartmann & Raymond 1989; Hartigan et al. 1995; Reipurth & Bally 2001). As a class, wTTs show very little evidence for a wind; the lack of an infrared excess indicates that they have already lost their disk. Thus the origin of [NII] and [SII] emission in our candidate wTTs is uncertain: If this emission is associated with these stars, the emission must be excited by some mechanism other than accretion. If the emission is not associated with these stars, a faint HII region in NGC 6871 is a plausible alternative source of forbidden line emission. Our test for nebular background emission in Section 4 appears to rule out this source of emission, but high resolution spectra would provide a better test.

We thank the Fred Lawrence Whipple Observatory staff and A. Mahdavi, K, Rines, E. Falco, W. Brown for helping with the observations and Susan Tokarz and the SAO Telescope Data Center for assistance in the data reduction. Comments from an anonymous referee improved our presentation.

REFERENCES

Aller L.H. 1943 ApJ, 97, 135

Arenou, F., Grenon, M., and Gomez, A. 1992 A&A, 258, 104

Cutispoto, G., Pastori, L., Tagliaferri, G., Messina, S., and Pallavicini, R. 1999 A&AS138, 87

Bernabei, S., and Polcaro, V.F. 2001 A&A, 366, 817

Battinelli, P., and Capuzzo-Dolcetta, R. 1991 MNRAS, 249, 76

Bertout, C. 1989 ARA&A, 27, 351

Bragg, A., and Kenyon, S.J. 2002 AJ, submitted

Fabricant, D., Cheimets, P., Caldwell, N. and Geary, J. 1998 PASP, 110, 79

Fitzgerald, M. P. 1968 AJ, 73 , 983

Garmany, C. D., and Stencel, R. E. 1992 A&AS, 94, 211

Gregorio-Hetem, J., Lepine, J. R. D., Quast, G. R., Torres, C. A. O., and de la Reza, R. 1992 AJ, 103, 549

Grigsby, J. A., and Morrison N. D. 1988 PASP, 100, 830

Habing, H. J., Dominik, C., Jourdain de Muizon, M., Laureijs, R. J. and Kessler, M. F., Leech, K., Metcalfe, L., Salama, A., Siebenmorgen, R., Trams, N., and Bouchet, P. 2001 A&A, 365, 545

Haisch, K.E. Lada, E.A. Lada, C.J. 2001 ApJ, 553, 153

Hakkila, J., Myers, J. M., and Stidham, B. J. 1997 AJ, 114, 2043

Hartigan, P., Edwards, S., and Ghandour, L. 1995 ApJ, 452, 736

Hartmann, L., and Raymond, J. C. 1989 ApJ, 337, 903

Hartmann, L., Calvet, N., Gullbring, E,. and D'Alessio, P. 1998, ApJ, 495, 385

Henry, T.J., Walkowicz, L.M., Barto, T.C., and Golimowski, D.A. 2002 AJ, 123, 2002

Hiltner, W.A. 1956 ApJS, 2, 389

Jacoby, G.H., Hunter, D.A., and Christian, C.A. 1984 ApJS, 56, 257

Jaschek, C., and Jaschek, M. 1987, The Classification of Stars (Cambridge University Press)

Joy, A.H., and Abt, H.A. 1974 ApJS, 28 ,1

Kenyon, S. J., and Hartmann, L. 1995 ApJS, 101, 117

Kenyon, S. J., Brown, D. L., Tout, C. A., and Berlind, P. 1998 AJ, 115, 2491

Lada, C.J., and Adams, F.C. 1992 ApJ, 393, 278

Mamajek, E. E., Lawson, W. A., and Feigelson, E. D. 1999 ApJ, 516, L77

Massey P., Johnson K. E., and DeGioia-Eastwood K. 1995 ApJ, 454, 151

Mermilliod, J-C. 1995, in "Information & On-Line data in astronomy,, Eds D. Egret and M.A. Albrecht, Luwer Academic Publishers(Dodrecht), p. 127

Neckel, T., and Klare, G., and Sarcander, M. 1980 A&AS, 42,251

O'Connell, R. W. 1973 AJ, 78, 1074

Osterbrock, D. E. 1989, Astrophysics of Gaseous Nebulae and Active Galactic Nuclei (Mill Valley, CA, University Science Books)

Reimann, H.G. 1989 Astron. Nachr. 310, 273

Reipurth, B., and Bally, J. 2001 ARA&A, 39, 403

de la Reza, R., Torres, C., Quast, G., Castilho, B., and Vieira, G. 1989 ApJ, 343, L61

Roman, N.G. 1951 ApJ, 114, 492

Schaller, G., Schaerer, D., Meynet, G., and Maeder, A. 1992 A&AS96, 269

Siess, L., Dufour, E., and Forestini, M. 2000 A&A, 358, 593

Slesnick, C. L., Hillenbrand, L. A., and Massey P. 2002 ApJ, accepted

Spangler, C., Sargent, A. I., Silverstone, M. D., Becklin, E. E., and Zuckerman, B. 2001 ApJ, 555, 932

Walborn, N.R. 1971 ApJS, 23, 257

Walter, F.M. 1987 PASP, 99, 31

Walter, F.M., Brown, A., Mathieu, R.D., Myers, P. C., and Vrba, F. J.1988 AJ, 96 297

Worthey, G., Faber, S.M., Gonzales, J.J., and Burnstein, D. 1994 ApJS, 94, 687

Zuckerman, B., Webb, R., Schwartz, M., and Becklin, E. 2001 ApJ, 549, L233

This preprint was prepared with the AAS LaTeX macros v5.0.

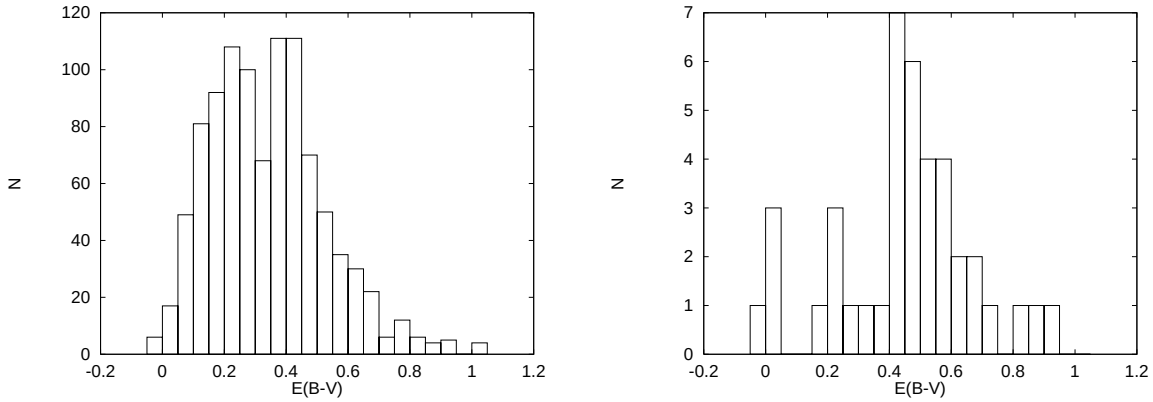

Fig. 2.— Histogram of the reddening for normal main sequence stars (left panel) and emission line stars (right panel) on the field of NGC6871

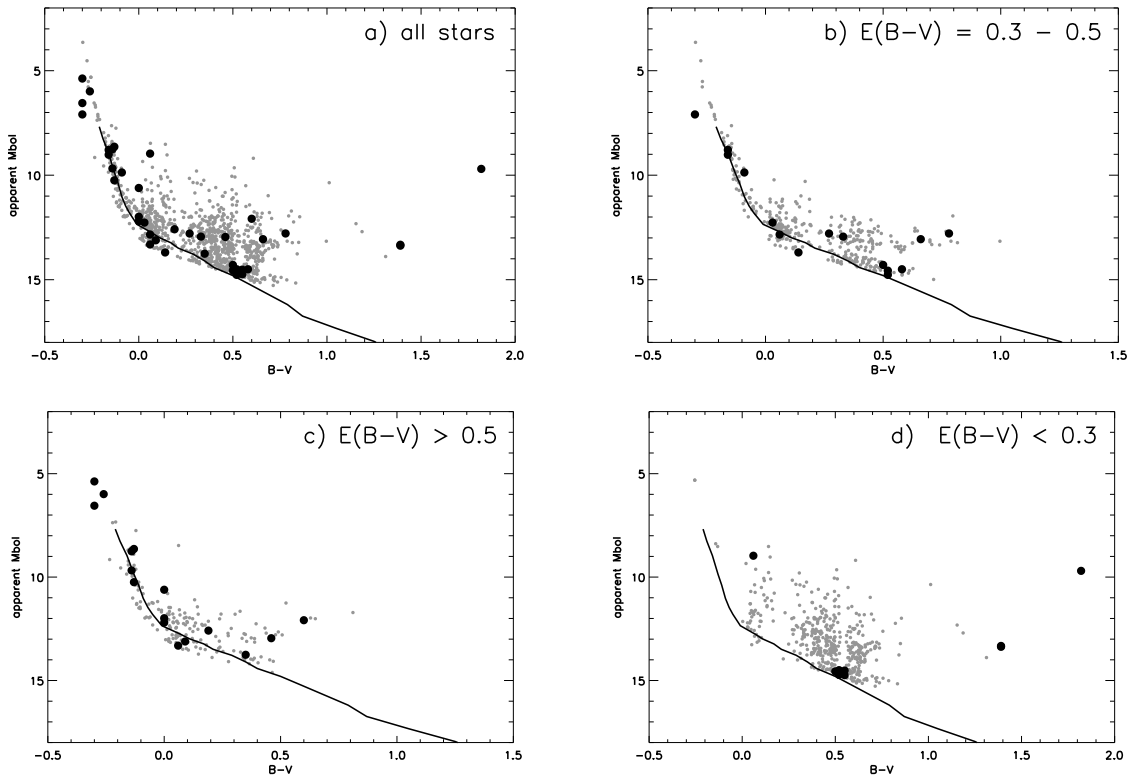

Fig. 3.— HRDs of different subsamples of NGC 6871 based on the photometry of Massey et al. (1995). Top left: all stars, top right: stars with $E(B-V)$ between 0.3 and 0.5, bottom left: stars with $E(B-V) > 0.5$, bottom right: stars with $E(B-V) < 0.3$. Small grey dots: normal main sequence stars, large black dots: emission line stars. The line represents the ZAMS of Siess et al. (2000) shifted with DM=11.0

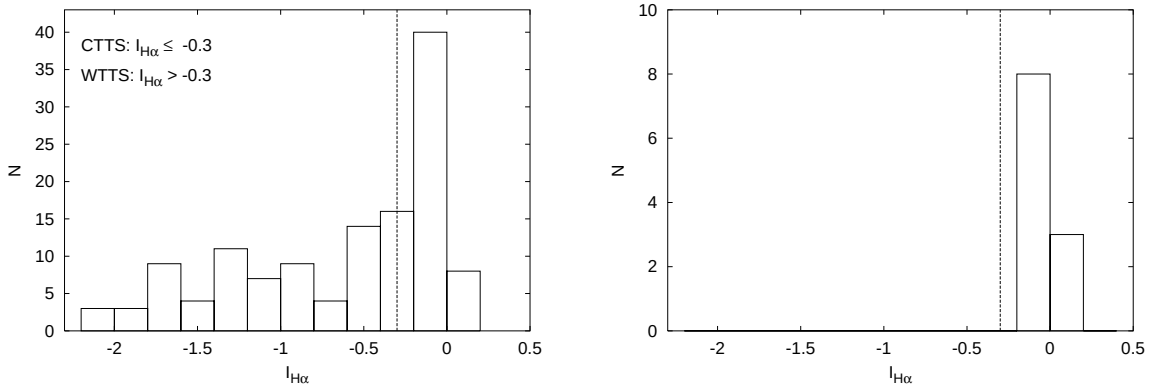

Fig. 4.— Histogram of the $H\alpha$ indices of late type PMS stars in the Taurus -Auriga molecular cloud (left panel) and our late type PMS candidates (right panel). The vertical dashed line denotes the boundary between the cTTs and wTTs stars

Table 1. Absorption indices used for measuring spectral types

Index name	central wavelength	bandwidth	blue sideband	red sideband
CN1	4160.875	35.00	4100.125	4265.375
CN2	4160.875	35.00	4091.375	4265.375
Caλ4227	4229.750	12.50	4216.625	4247.250
Gλ4300	4300.125	35.00	4275.750	4328.250
Feλ4383	4396.000	51.25	4366.000	4450.375
Caλ4455	4464.625	22.50	4451.500	4485.875
Feλ4531	4538.000	45.00	4510.500	4571.125
Feλ4678	4678.375	86.25	4622.125	4750.875
Hβ	4861.250	28.75	4837.875	4884.125
Feλ5015	5015.875	76.25	4962.125	5059.625
Mg1	5101.625	65.00	4926.375	5333.625
Mg2	5173.875	39.50	4926.375	5333.625
Mgb	5176.375	32.50	5152.000	5198.875
Feλ5270	5265.650	40.00	5240.650	5301.900
Feλ5335	5332.125	40.00	5310.250	5358.375
Feλ5406	5401.250	27.50	5381.875	5420.000
Feλ5709	5710.250	23.75	5686.500	5731.500
Feλ5782	5788.375	20.00	5772.125	5806.500
NaD	5894.875	32.50	5869.875	5936.875
TiOλ5968	5968.3	40	5835.6	6073.3
TiOλ6234	6233.7	40	6106.5	6396.8
Hα	6565	30	6330	6600
Hβ	4861	20	4785	5050
Hγ	4340	20	4270	4400
Hδ	4101	20	4015	4270
Hλ3889	3889	20	3860	3910
Hλ3835	3835	20	3815	3860
Heλ4144	4144	20	4063	4175
Heλ4387	4387	20	4370	4510
Heλ4471	4471	20	4370	4510
Heλ4026	4026	20	3995	4063
Heλ4922	4922	20	4900	4950
CaII	3933	20	3910	4015

Table 1—Continued

Index name	central wavelength	bandwidth	blue sideband	red sideband
Mgλ5175	5175	30	5050	5300
Naλ5892	5892	30	5820	6100
CHλ4305	4305	20	4270	4400
Baλ6495	6495	30	6330	6620
TiOλ6180	6182	40	6127	6372
TiOλ7100	7100.5	40	7050	7400

Table 2. Stars with certain $H\alpha$ emission in NGC 6871. The photometric data are from Massey et al. (1995).

Id	SIMBAD Id	V	B-V	U-B	Sp. Type (present paper)	Sp. Type (literature)	$I_{H\alpha}$	E(B-V)	evol. stat.	first reported
0001	HD 190918	6.83	0.11	-0.74	-	WN5 + O9.5 III	-0.282791	> 0.41	super-giant	Aller (1943)
0006	HD 227611	8.74	0.31	-0.67	B0	B0 II:pe	-1.411940	0.61	giant	Hiltner (1956)
0008	SAO 69404	8.85	0.17	-0.53	B0	B0.5 Ve	-0.004206	0.47	MS	Grigsby & Morrison (1988)
0186	Cl* NGC 6871 BP 2	11.98	0.32	-0.13	B4	B5 Ve	-0.357927	0.48	MS	Bernabei & Polcaro (2001)
2352	Cl* NGC 6871 BP 3	12.75	0.38	-0.09	B5	B8 Ve	-0.333665	0.52	MS	Bernabei & Polcaro (2001)
2905	HD 226868	8.81	0.83	-0.29	O9	O9.7 Iab	-0.042580	> 1.13	super-giant	Massey et al. (1995)
0215	[MJD95] J200700.98+354006.3	10.27	0.25	-0.51	B1		-0.168169	0.51	MS	present paper
2209	[MJD95] J200512.93+355113.3	13.13	0.80	0.14	B5		0.003828	0.94	PMS	present paper
1062	[MJD95] J200728.78+354632.8	11.71	0.47	-0.58	B6		-0.507890	0.6	PMS	Massey et al. (1995)
1238	[MJD95] J200711.83+353853.3	13.47	0.52	0.16	B6		-0.023224	0.65	MS	present paper
0038	[MJD95] J200547.79+353811.4	11.91	0.31	0.06	B8		0.098522	0.4	PMS	present paper
2320	[MJD95] J200453.31+353646.8	14.70	0.71	0.42	A0		-0.183464	0.71	PMS	present paper
2492	[MJD95] J200418.58+355426.0	13.02	0.68	0.45	A0		-0.038215	0.68	PMS	present paper
2139	[MJD95] J200522.04+353719.8	13.83	0.46	0.20	A1		0.251928	0.43	PMS	present paper
2399	HD 227480	9.26	0.09	-0.04	A2	A3 II	0.160104	0.03	MS	present paper
1694	[MJD95] J200615.06+354101.4	14.41	0.76	0.36	A9		0.177453	0.49	PMS	present paper
2646	[MJD95] J195957.80+351908.6	15.88	0.96	0.47	F7		-0.104228	0.46	PMS	present paper
2631	[MJD95] J200002.77+351856.2	16.03	0.94	-0.11	F8:		-0.109664	0.42	PMS	present paper
2055	[MJD95] J200532.16+353809.0	15.95	0.85	0.35	F8:		-0.604574	0.33	MS	present paper
1755	[MJD95] J200608.03+354011.6	15.31	0.73	0.17	F8		0.082073	0.21	PMS	present paper
1552	[MJD95] J200631.73+353609.9	15.37	0.77	0.32	F9		-0.077949	0.22	MS	present paper
2675	[MJD95] J195948.26+352142.9	15.92	0.98	0.38	G0:		0.035220	0.4	PMS	present paper
2245	[MJD95] J200508.36+353708.5	13.98	1.15	0.25	G1		-0.028562	0.55	PMS	present paper
2621	[MJD95] J200006.39+351402.8	14.79	1.15	0.82	G5		-0.020041	0.49	PMS	present paper
2138	[MJD95] J200522.08+354212.0	14.40	1.21	0.87	G9		-0.019457	0.43	PMS	present paper
1286	[MJD95] J200705.96+355110.7	14.08	1.48	1.29	K2		0.000891	0.59	giant	present paper
1647	[MJD95] J200621.20+355600.6	14.42	1.41	1.05	K8		-0.081935	0.02	PMS	present paper
1659	[MJD95] J200619.32+355546.4	14.37	1.38	0.86	K8		-0.073231	-0.01	PMS	present paper

Table 3. Emission line candidate stars in NGC 6871. The photometric data are from Massey et al. (1995)

Id	MJD95 Id	V	B-V	U-B	Sp. Type (present paper)	Sp. Type (literature)	$I_{H\alpha}$	E(B-V)	evol. stat.	first reported
2	HD 190919	7.29	0.25	-0.62	O9	B1 Ib	0.085103	> 0.55	super-giant	present paper
3	SAO 69403	7.38	0.25	-0.64	B0	B1 Ib	0.082967	0.55	super-giant	present paper
2092	[MJD95] J200557.85+354721.1	11.93	0.23	-0.07	B4		0.154545	0.39	MS	present paper
1651	[MJD95] J200622.09+354847.8	13.90	0.52	0.34	A0		0.240811	0.52	PMS	present paper
1980	[MJD95] J200544.49+355352.3	14.34	0.48	0.23	A2		0.277399	0.42	MS	present paper
1093	[MJD95] J200725.36+353633.7	16.15	0.91	0.29	A2		0.287980	0.85	MS	present paper
2637	[MJD95] J200000.73+352316.3	15.02	0.65	0.46	A3		0.298494	0.56	MS	present paper
1710	[MJD95] J200613.34+355244.8	15.24	0.59	0.31	A5:		0.245813	0.45	PMS	present paper
2156	[MJD95] J200519.35+354222.6	14.35	0.72	0.44	A7		0.210561	0.53	PMS	present paper
2067	[MJD95] J200529.55+354551.7	14.31	0.74	0.55	F1		0.165404	0.41	PMS	present paper
1379	[MJD95] J200656.29+354947.8	16.47	1.19	-0.85	F2		0.129417	0.84	PMS	present paper
1845	[MJD95] J200559.51+355137.2	14.81	1.01	0.34	F6		0.099795	0.55	PMS	present paper
1221	[MJD95] J200714.35+355322.2	15.18	0.65	0.21	F7		0.090169	0.15	MS	present paper
2545	[MJD95] J200408.60+355006.3	15.63	0.76	0.06	F8		0.102688	0.24	MS	present paper
1869	[MJD95] J200556.66+354229.7	15.75	0.82	0.10	F9		0.076941	0.27	MS	present paper
113	[MJD95] J200608.60+353458.1	13.02	1.83	1.97	M5:		-0.022871	0.01	PMS	present paper